DYNAMIC CRUSH TEST ON HYDROGEN PRESSURIZED CYLINDER

Hiroyuki Mitsuishi[1], Koichi Oshino[2], Shogo Watanabe [2]
[1] Japan Automobile Research Institute, Takaheta1328-23, Shirosato, Ibaraki, 311-4316, Japan
[2] Japan Automobile Research Institute, Karima2530, Tsukuba, Ibaraki, 305-0822, Japan

ABSTRACT

It is necessary to investigate cylinder crush behavior for improvement of fuel cell vehicle crash safety. However, there have been few crushing behavior investigations of high pressurized cylinders subjected to external force. We conducted a compression test of pressurized cylinders impacted by external force. We also investigated the cylinder strength and crushing behavior of the cylinder. The following results were obtained.

1) The crush force of high pressurized cylinders is different from the direction of external force. The lateral crush force of high pressurized cylinders is larger than the external axial crush force.

2) Tensile stress occurs in the boundary area between the cylinder dome and central portion when the pressurized cylinder is subjected to axial compression force, and the cylinder is destroyed.

3) However, the high pressurized cylinders tested had a high crush force, which exceeded the assumed range of vehicle crash test procedures.

1. INTRODUCTION

From the viewpoint of environmental measures and the prevention of global warming by reduction of carbon dioxide emissions, industry, academia, and government in Japan are all advancing research for the development and spread of fuel cells, which use hydrogen as fuel and emit no harmful substances. The government is also leading efforts to research and develop various safety assessment methods in anticipation of the widespread use of fuel cell vehicles. For the development and spread of clean fuel cell vehicles, the Japan Automobile Research Institute (JARI) has been commissioned by the New Energy and Industrial Technology Development Organization (NEDO) since 2000 to study the performance and safety of fuel cell vehicles [1][2][3].

Since we had little experience with vehicles loaded with hydrogen fuel, we began these studies on the safety of fuel cell vehicles with an examination focused on the technology for storing hydrogen in a vehicle, assuming the worst situation of a vehicle collision. Since high pressure hydrogen tanks are currently the method of hydrogen storage that is nearest to practical application for automobiles, we studied the case in which an onboard high pressure hydrogen tank is subjected to direct external force such as in a vehicle collision. Our studies have covered matters that had not been previously examined, including the strength of high pressure fuel tanks subjected to such pressure, weak points in the way force is applied, the crushing behavior exhibited when a tank is crushed by an external force, and the surrounding damage that can be expected [4].

From among a series of external force destruction tests on high pressure tanks, we describe herein the results of dynamic external force destruction tests that investigated the crush behavior of cylinders filled with high pressure gas, in which a weight was dropped from above.

2. DYNAMIC GAS PRESSURIZED EXTERNAL FORCE DESTRUCTION TEST

2.1 Test methods and measurements

These tests were falling weight impact tests in which a high pressure tank was forcibly crushed. This was done by dropping a weight with a mass of 2.5 tons from a height of 2.0 m onto high pressurized cylinders filled with either helium or hydrogen gas (Fig. 1). The impact energy of 49,000 J in this test is equivalent to that in a collision of a vehicle with mass of 1 ton traveling at a velocity of about 36 km/h.

Items recorded included crushing load, weight acceleration, tank internal pressure, deformation in various locations, high speed video, and blast probe.

The test parameters in the dynamic gas pressurization external force destruction test were load conditions (vertical, horizontal directions), filling pressure (7 MPa: pressure below the rupture stress of the aluminum liner body, 35 MPa: maximum filling pressure), displacement magnitude (target values: 50 mm, 100 mm), filling gas (hydrogen, helium), boss neck length (standard, long), and cylinder (Type-3, Type-4) (Table 1). Displacement magnitude was set so that when the weight contacted the high pressure tank, the weight collides with a wooden stopper and is forcibly stopped at the point when the target displacement is reached.

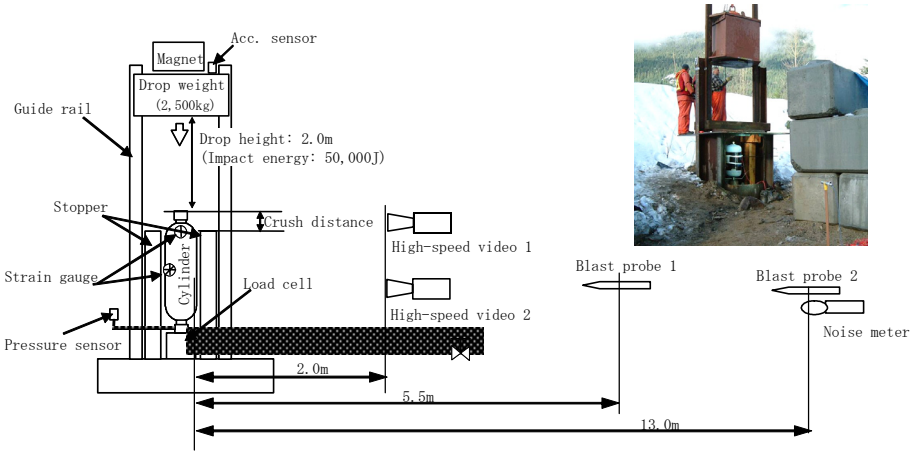

Figure 1. Diagrams of test conditions.

Table 1. Test conditions.

Disp. (mm)				50			100		
Test Cylinder				Type-3a	Type-3b	Type-4	Type-3a	Type-3b	Type-4
Situation	Gas	In-Press.	Neck Length						
Axial	He	7MPa	Normal				Test	Test	Test
		35MPa	Normal	Test	Test	Test	Test	Test	Test
		35MPa	Long				Test		
	H_2	35MPa	Normal				Tested (Ignited)		Test
Lateral	He	35MPa	Normal	Test					

Cylinder size: Type-3a:Dia.280mm, L960mm, Type-3b:Dia.432mm, L1050mm
Type-4:Dia.400mm, L915mm

2.3 Experimental results

Table 2 summarizes the results for the destruction shape of the tank in the dynamic gas pressurization external force destruction tests. When the destruction morphology of the tank comprised axial pressure for the load morphology, high internal pressure, and high displacement magnitude, some tanks were seen to burst. When the filling gas was hydrogen, a case of fire was seen.

Table 2. Test results.

Disp. (mm)				50			138	100	
Test Cylinder				Type-3a	Type-3b	Type-4	Type-3a	Type-3b	Type-4
Situation	Gas	In-Press.	Neck Length						
Axial	He	7MPa	Normal				T-3: leak	T-10: leak	T-9: leak
		35MPa	Normal	T-2(88mm): rupturte T-8(retake): rupturte	T-11: leak	T-5: leak	T-1: rupture	T-12: leak	T-6: rupture
		35MPa	Long				T-4: rupture		
	H_2	35MPa	Normal				Tested (rupture) (ignite)		T-13: rupture
Lateral	He	35MPa	Normal	T-7(25mm): non leak					

T-number: test number

(1) Cases of tank burst as destruction morphology

Images from a high speed video taken during test T-2 (cylinder: Type-3a, filling pressure: 35 MPa, load morphology: axial compression, displacement magnitude: 88 mm) are shown in Fig. 2. The images are of the top dome of the dome portion where the deformation was concentrated. The time when the weight and boss make contact is taken to be 0 ms, and the images are at 4 ms intervals. The tank boss is the contact surface, and after it comes in contact with the flat surface of the weight, the mouth ring collapses into the tank dome, and 13 ms later the tank bursts. Figure 3 shows the condition around the cylinder before and after the test.

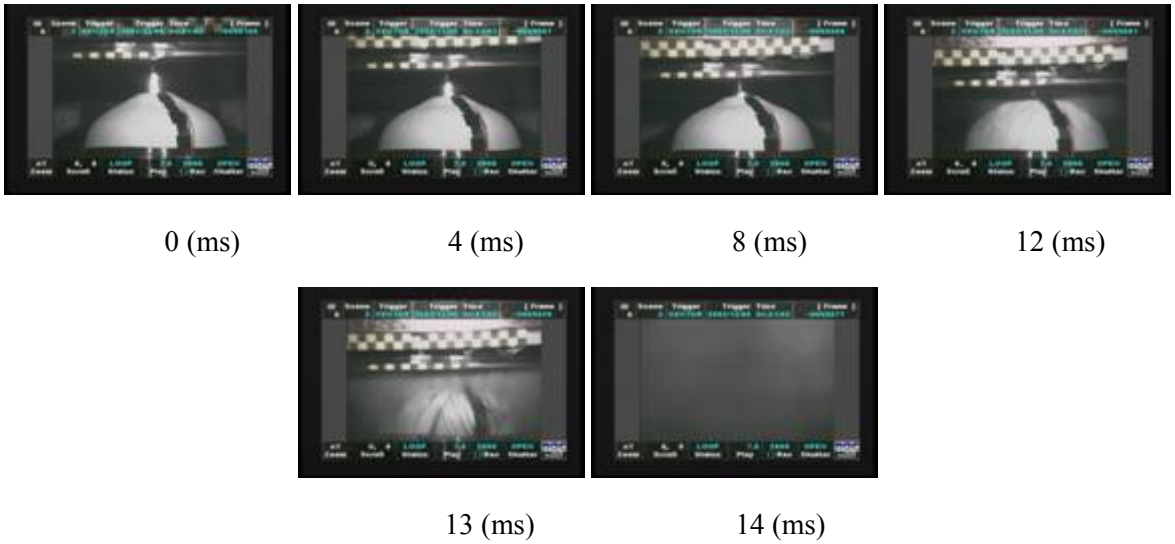

Figure 2. High-speed video (T-2: Type-3a, Axial, Disp. 88 mm, 35 MPa).

before after

Figure 3. Cylinder situation (T-2: Type-3a, Axial, Disp. 88 mm, 35 MPa).

The cylinder fixed in position before the test, was ruptured at the border of the body and dome sections of the cylinder after the test. It was thrown out of the test apparatus by the impact. The force-displacement curve from the test is shown in Fig. 4.

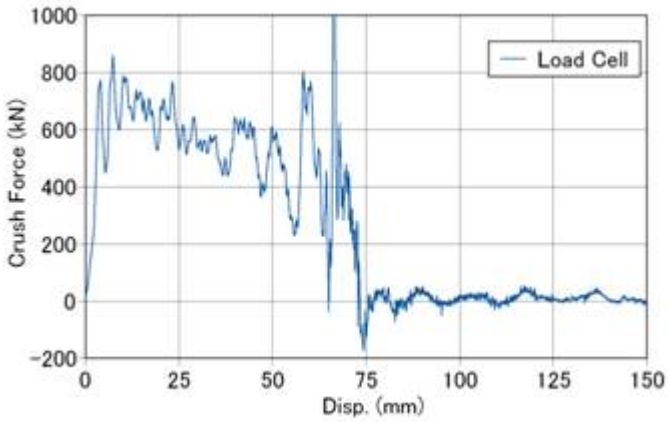

Figure 4. Force – displacement curve (T-2: Type-3a, Axial, Disp. 88 mm, 35 MPa).

During the crush, a load of about 800 kN is generated in the cylinder with the initial deformation, and then at a displacement of about 60 mm, a high load is again generated. Afterward, the cylinder ruptures at a displacement of about 65 mm. Considering at the rigidity of the high pressure tank filled with fuel, it is seen that in automobile crash tests, the barrier load at the time of full wrap anterior wrap crash tests shows the maximum load, but even with that barrier load, the level is less that 800 kN. Therefore, under the conditions of the automobile crash test method, the high pressure tank filled with fuel maintains a sufficient rigidity, and the possibility of a tank rupture occurring is extremely low.

Next, the pressure measured by blast probes located 5.5 m and 13 m away from the tank center, are shown in Fig. 5.

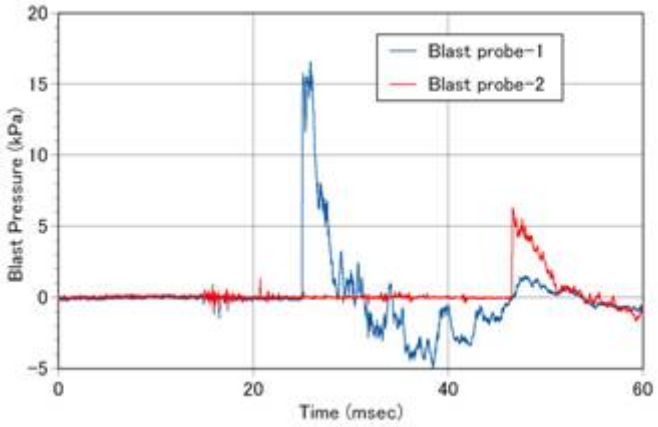

Figure 5. Blast pressure – time curve (T-2: Type-3a, Axial, Disp. 88 mm, 35 MPa).

The pressure of probe 1 located at a point 5.5 m from the tank was a maximum of around 15 kPa. From the distances of probes 1 and 2 and the time when pressure waves were measured, it was determined that the pressure waves spread in the vicinity at approximately the velocity of sound.

(2) Cases of leak as destruction morphology

Figure 6 shows high speed video images for test T-3 (cylinder: Type-3a, filling pressure: 7 MPa, load morphology: axial compression, displacement magnitude: 138 mm), which was conducted at an internal pressure below the rupture stress of the aluminum liner.

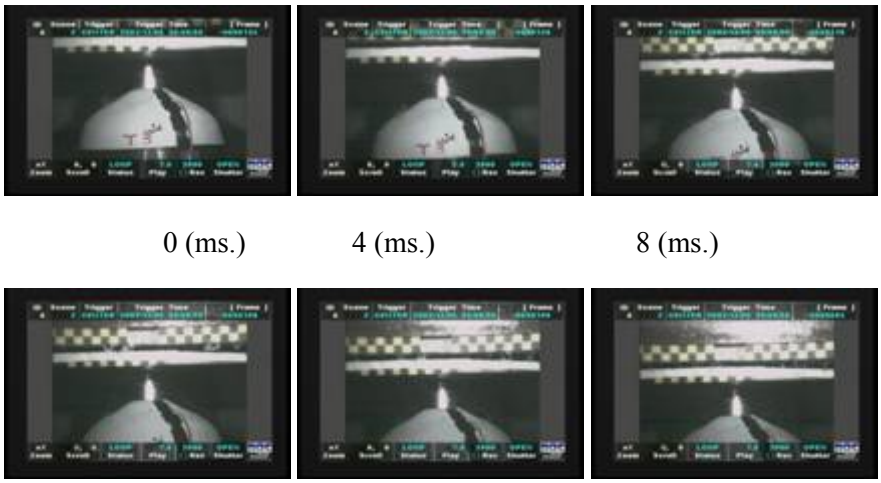

0 (ms.) 4 (ms.) 8 (ms.)

12 (ms.) 16 (ms.) 20 (ms.)

Figure 6. High-speed video (T-3: Type-3a, Axial, Disp. 138 mm, 7 MPa).

With an internal pressure of 7 MPa, after contact between the weight and boss, the boss simply collapsed into the dome and no rupture of the cylinder was seen within a time up to 20ms. Figure 7 shows the force-displacement curve with an internal pressure of 7 MPa.

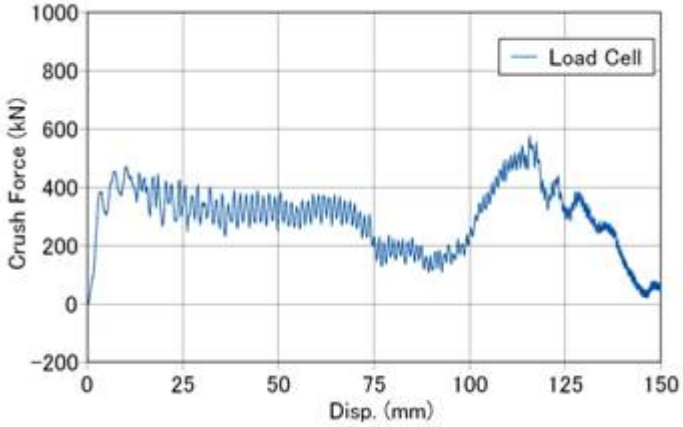

Figure 7. Force – displacement curve (T-3: Type-3a, Axial, Disp. 138 mm, 7 MPa).

With an internal pressure of 7 MPa, the load during the initial deformation shifted to the level of 400 kN, and the peak load of 500 kN occurred at a displacement of about 115 mm. The pressure measured by blast probes located 5.5 m and 13 m from the center of the cylinder with the internal pressure of 7 MPa is shown in Fig. 8.

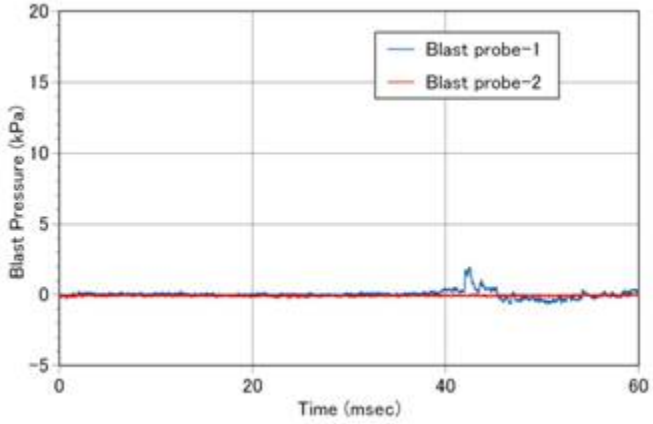

Figure 8. Blast pressure – time curve (T-3: Type-3a, Axial, Disp. 138 mm, 7 MPa).

With the internal pressure of 7 MPa, pressure waves of a level that would be expected to cause damage were not measured by either probe 1 or 2.

(3) Test examples with different cylinders

Figure 9 shows the condition before and after test T-12 (cylinder: Type-3b, filling pressure: 35 MPa, load morphology: axial compression, displacement magnitude: 100 mm), which used the same type of cylinder (Type-3: aluminum alloy with full wrap liner) as in the previous tests, but has different specifications such as the thickness of the aluminum liner. A Type-3a cylinder ruptured under the same test conditions as in T-12.

before after

Figure 9. Cylinder situation (T-12: Type-3b, Axial, Disp. 100 mm, 35 MPa).

Damage to the cylinder after the test was concentrated around the dome, but no ruptures were seen in the border area between the cylinder dome and body. The force-displacement curve is shown in Fig. 10. The load showed a maximum value of about 75 kN in the initial deformation at about 20 mm, and afterward decreased. However, no load increase was seen immediately before rupture (Fig. 4) as was seen in examples of rupture.

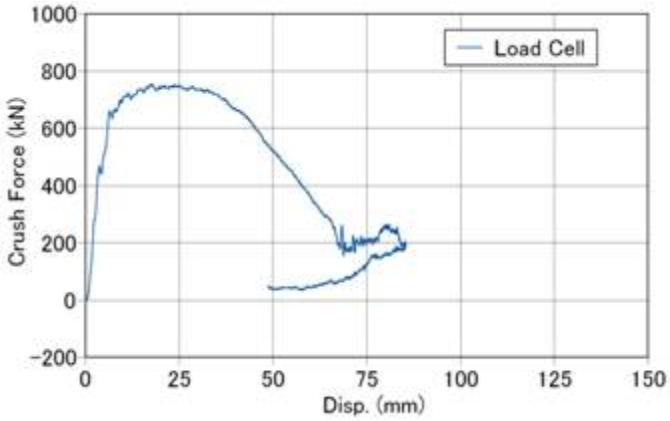

Figure 10. Force – displacement curve (T-12: Type-3b, Axial, Disp. 100 mm, 35 MPa).

Next, Fig. 11 shows the blast pressure measured by blast probes located 5.5 m and 13 m from the center of the cylinder in test T-12 (cylinder: Type-3b, filling pressure: 35 MPa, load morphology: axial load, displacement magnitude: 100 mm). With the Type-3b cylinder, no pressure waves of a level predicted to cause damage were measured.

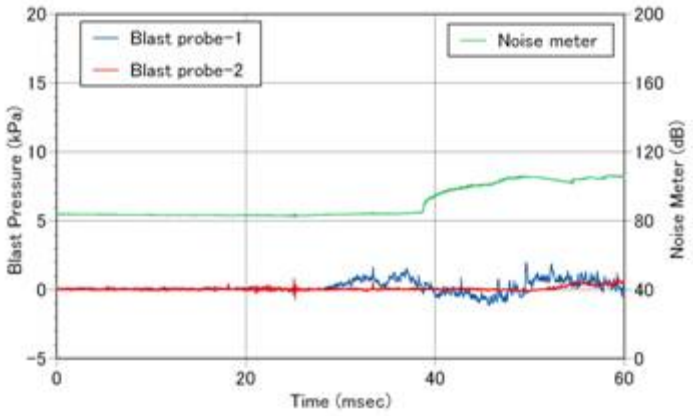

Figure 11. Blast pressure & noise meter – time curve (T-12: Type-3b, Axial, Disp. 100 mm, 35 MPa).

3. ANALYSIS OF DAMAGED PORTIONS OF CYLINDER

In tests in which the cylinder did not burst, damage was concentrated in the dome. Figure 12 shows the condition of the dome after test T-3, and Fig. 13 shows that after test T-12.

Exterior Interior of bottom dome Interior of top dome

Figure 12. Damage to cylinder in test T-3 (T-3: Type-3a, Axial, Disp. 138 mm, 7 MPa).

Exterior Interior of bottom dome Interior of top dome

Cross section of bottom dome Area around mouth ring of bottom dome

Figure 13. Damage to cylinder in test T-12 (T-12: Type-3b, Axial, Disp. 100 mm, 35 MPa).

In cases when the cylinder did not burst, the area around the mouth ring of the aluminum liner was damaged, and gas leaked from the damaged portions. However, since the damage did not extend to the cylinder body, there was no large-scale emission of filling gas as a result of fracture in the cylinder body. Next, Fig. 14 shows the fracture surface of the fractured portion of the cylinder in test T-2, in which the cylinder ruptured.

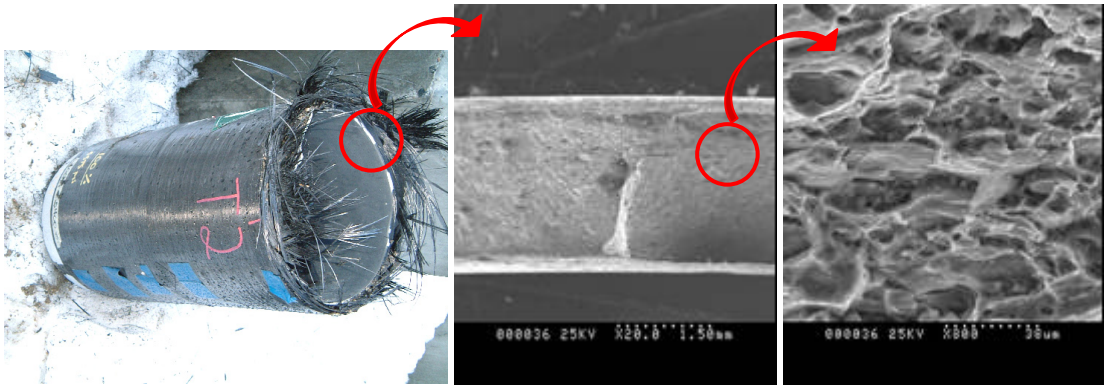

Fractured cylinder Fracture surface photo 1 Fracture surface photo 2 (magnification)

Figure 14. Fractured surface of burst cylinder (T-2: Type-3a, Axial, Disp. 138 mm, 35 MPa).

The cylinder fracture portion shows a clear tensile fracture surface. It was found the despite the compression of the cylinder by the weight, tensile stress acted in the fractured portion and the cylinder body fractured and

burst. In the force-displacement curve of test T-2 (Fig. 4), the load increased immediately before the cylinder burst, which occurred just after the peak load. However, since this peak load nearly corresponded with the tensile fracture load in the cylinder body, the cylinder fracture may be considered from the measurement data also to have occurred from the action of tensile stress on the cylinder body.

4. PROCESS OF CYLINDER FRACTURE

Based on the test and analysis results so far, the process through which the cylinder ruptures is summarized in Fig. 15.

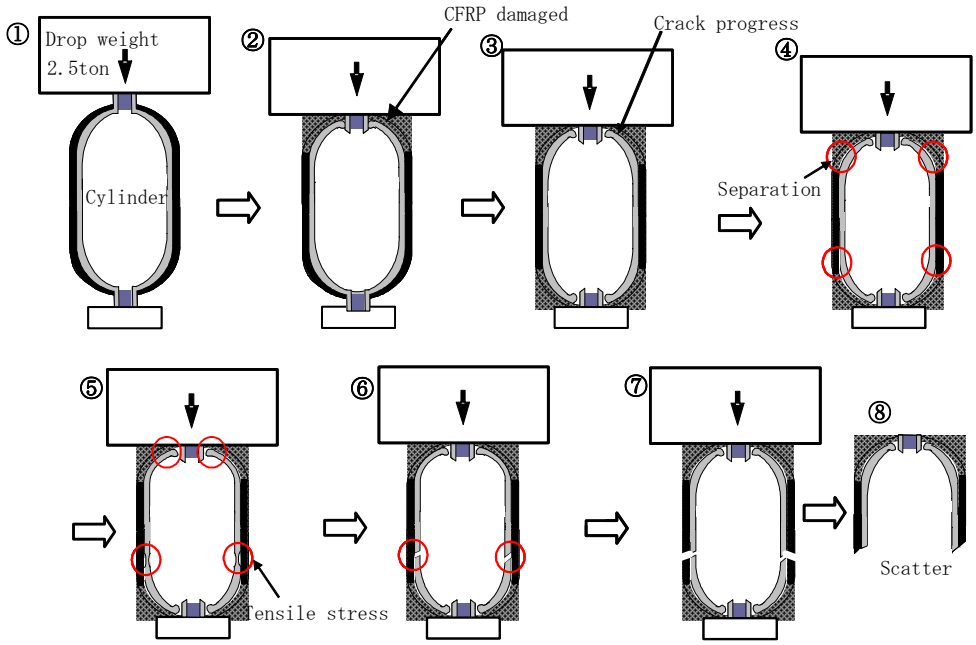

Figure 15. The cylinder ruptures process.

The theoretical process of the fracture in the dynamic gas pressurized external force destruction test is as follows:

1. Instant of weight impact

2. Deformation stress is concentrated around the boss in the portion receiving the impact (top dome), the boss collapses, and a crack develops from the boss toward the body.

3. The deformation load around the bottom dome boss is smaller than in the top dome, and the deformation shifts to the bottom dome

4. The aluminum liner is separated from CFRP in the top and bottom domes, and the aluminum liner is no longer be reinforced by the CFRP.

5. The aluminum liner of the top dome generates expansion space for the cylinder body as a result of crush deformation

6. The body aluminum liner that is not reinforced by CFRP (because of separation) cannot withstand the internal pressure, a circular fissure occurs for the reasons given above in the border area between the cylinder dome and body, and the cylinder fractures

7. In cases when there is some ignition source, the leaking hydrogen ignites. The crack produced from the boss toward the body on the bottom dome side advances and the cylinder fractures

8. The top dome/body and bottom dome rupture and fragments from the fracture fly in all directions

Thus, tensile stress occurs in the liner body as the cylinder is compressed by the weight, and the cylinder ruptures.

5. CONCLUSION

A series of dynamic gas pressurization external force destruction tests were conducted as a project for the basic development and spread of automobile fuel cell systems, commissioned by NEDO. The findings in these tests are summarized below.

1) Process until rupture

Based on the fracture analysis results (tensile fracture surface) and other findings, it is concluded that the ruptures seen in the present tests occurred after the separation of the CFRP reinforcement layer and aluminum liner layer from the pressure applied by the weight, when the stress on the aluminum liner from the internal pressure exceeded the fracture stress of the aluminum material.

2) Effect on surroundings

In the cases of leak, no pressure waves were generated and there was almost no effect on the surroundings. Conversely, in the cases of cylinder fracture pressure waves spread to the surroundings.

3) Standardization

The fracture load of high pressure cylinders is outside the presumed range in automobile collisions. Therefore, evaluation by means such as crash tests is thought to be unnecessary. However, the design factors for high pressure gas tanks currently have almost no standards for external force, and this remains an issue for discussion.

REFERENCES

1. Yohsuke Tamura, et al., The Fire Tests with High-Pressure Hydrogen Gas Cylinders for Evaluating the Safety of Fuel-cell Vehicles, *SAE International 2004-01-1013*.
2. Hiroyuki Mitsuishi, et al., Study on Fue Leakage Measurement System of Fuel Cell Vehicles, 18th International Technical Conference on the Enhanced Safety of Vehicles, 2003.
3. Yoshiyuki Hashimasa, et al., Study of Fuel Cell Structure and Heating Method for the Standardization of Single Cells, 2004 Fuel Cell Seminar, 2004.
4. Hiroyuki Mitsuishi, et al., Compression Characteristics of High-Pressure Cylinders for Vehicles, JARI Research Journal, 2002(In Japanese).